PROCEEDINGS OF SCIENCE

Detection of Extensive Air Showers with the self-triggered TREND radio array

Sandra Le Coz*[1], Didier Charrier[5], Krijn D. de Vries[6], Quanbu Gou[2], Junhua Gu[1], Hongbo Hu[2], Olivier Martineau-Huynh[3], Clementina Medina[3], Valentin Niess[4], Matías Tueros[7], Xiangping Wu[1], Jianli Zhang[1], Yi Zhang[2]

[1] *National Astronomical Observatory of China, Chinese Academy of Sciences, Beijing 100012, China*
[2] *Key Laboratory of Particle Astrophysics, Institute of High Energy Physics, Chinese Academy of Sciences, Beijing 100049, China*
[3] *LPNHE, CNRS-IN2P3 and Universités Paris 6 & 7, BP200, 4 place Jussieu, 75252 Paris, France*
[4] *LPC, CNRS-IN2P3, Université Blaise Pascal, BP 10448, 63000 Clermond-Ferrand, France*
[5] *SUBATECH, CNRS-IN2P3, Université de Nantes, Ecole des Mines de Nantes, Nantes, France*
[6] *Vrije Universiteit Brussel, Dienst ELEM, B-1050 Brussels, Belgium*
[7] *Instituto de Física La Plata, CONICET CCT-La Plata, Calle 49 esquina 115 (1900), La Plata, Argentina*
E-mail: lecozsandra@yahoo.com

We demonstrate here the ability of TREND, a self-triggered antenna array, to autonomously detect and identify air showers induced by cosmic rays, from their radio emission, measured in the 50-100 MHz frequency range. TREND (Tianshan Radio Experiment for Neutrino Detection) is an array of 50 single polarised antennas, deployed over a total area of 1.5 km^2 on the site of the 21 cmA radio interferometer in the radio-quiet Tianshan mountains (China), that was running between 2011 and 2013. The TREND DAQ system was designed to allow for a trigger rate of up to 200 Hz per antenna, based on a very basic signal-over-threshold trigger condition. The reconstruction and discrimination of air showers from the ultra-dominant background noise is then performed through an offline treatment.

We present here, for the first time, a detailed search for extensive air showers with the TREND data. We first explain the background-rejection algorithm which allowed to select about 500 air shower radio candidates from the $\sim 7.10^8$ radio pulses recorded with the TREND array. We then show that the distribution of the directions of arrivals of these $\sim$500 candidates is compatible with what is expected for air showers. We finaly compute the TREND air shower detection efficiency, thanks to an end-to-end simulation chain which will be detailed here. Given the fairly basic TREND data acquisition chain, these results can be considered extremely encouraging in the perspective of future experiments using radio as a way to detect air showers, such as the Giant Radio Array for Neutrinos Detection.

35th International Cosmic Ray Conference - ICRC2017
10-20 July, 2017
Bexco, Busan, Korea

*Speaker.

PoS(ICRC2017)406

1. Introduction

Radio detection of extensive air showers has made significant progress since the 2000's. Today, data from antenna arrays is used to perform air shower direction and energy reconstruction [1, 2], but autonomous detection is still a challenge. Indeed, because of high electromagnetic environmental noise and consequently a high deadtime of the electronics, radio detection experiments are generally based on external triggering using particle detectors. We show here the ability of TREND to detect air showers in a stand-alone mode.

2. Setup

TREND (Tianshan Radio Experiment for Neutrinos Detection) consists of 50 butterfly antennas with a 150 m spacing, it covers 1.5 km^2. It is located in the Tianshan area in northern China (Xin Jiang province), on the site of the "21 cmA" astrophysics experiment facilities. TREND was proposed in 2008, as a collaboration between France and China [3]. The goal was to establish the autonomous radio detection of extensive air showers. Because of the low electromagnetic noise in the Tianshan area, it is a perfectly suitable location to reach this goal.

The 50 butterfly antennas are single arm antennas, they are therefore sensitive to a single polarisation. The arms were orientated along the East-West direction in 2011 and 2012, and along the North-South direction in 2013. The antenna is 130 cm long and 50 cm wide, set up 1.5 m above the ground. The radius of its wires is 5 mm. Each antenna is connected to a transformer, to several amplifiers for a total gain of 64 dB, and to frequency filters (50-100 MHz). The electric signal of the antenna is passed through a coaxial cable to the nearest 21 cmA station (less than 300 m away) where it is converted to light to reach the DAQ room (less than 2 km away) through optical fibers. The signal is then digitized at 200 MS/s using 8-bits ADCs. If a transient signal reaches an amplitude above 6 or 8 σ from the baseline, a T0 trigger is issued. If 4 or more antennas get a T0 tag in causal coincidence, a subset of 5 μs around the trigger time position is saved to disk. This is an "event". Picture 1 shows the TREND layout, one of the antennas and one of the recorded signals.

3. Data analysis

About 7.10^8 events were recorded to disk in the 316 data acquisition days of the East-West orientation period. The offline analysis program performs the directional reconstruction of these events. Then it applies successive cuts which are based on extensive air shower expectations: pulse shape, multiplicity (number of antennas in the event) >5, trigger pattern at ground, valid directional reconstruction, curvature of the wavefront, and direction and time correlation between events. Indeed, the signal is expected to be short and to faint promptly when moving away from air shower axis. Also, we do not expect many events from the same origin in a short range of time, while this is a typical behiavior of noise sources, because they are often static and emit in bursts.

This treatment allows to select 574 air shower candidates from the $\sim 7.10^8$ recorded events (background dominated). Statistically, the angular distribution of these candidates is expected to show an overdensity for directions normal to the geomagnetic field, because, at first order, the intensity of the radio emission increases as the air shower is more perpendicular to the geomagnetic

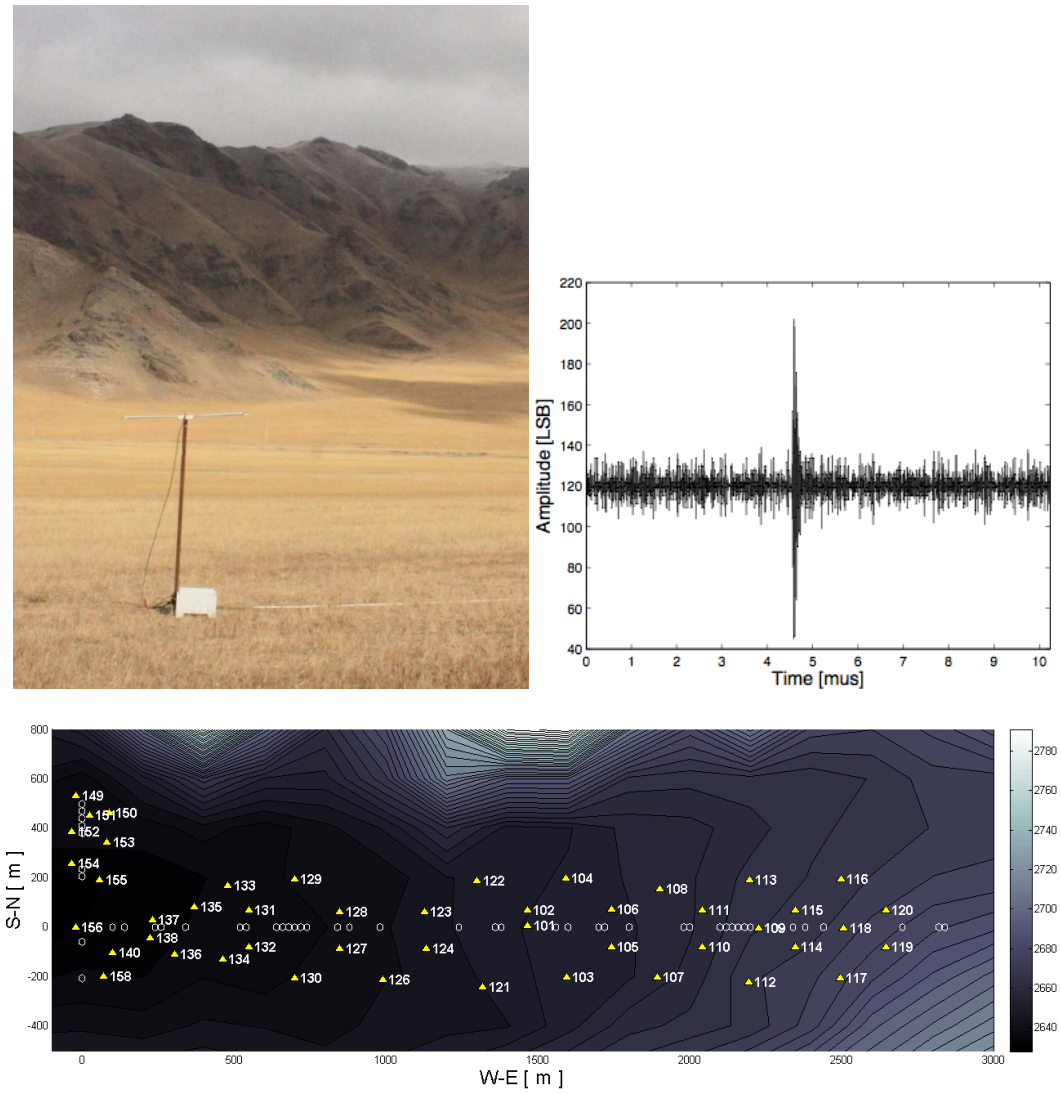

Figure 1: One TREND antenna (top left), one TREND recorded signal (top right), TREND layout (bottom).

field. As depicted in figure 2, the angular distribution for the 574 candidates shows a good agreement with expectations. However, in order to perform a more quantitative interpretation of this result, it is necessary to make an end-to-end simulation of the TREND response to air showers. This is detailed in section 5. In section 4, we explain how we calibrate the TREND data acquisition chain, which is an essential ingredient to this end-to-end simulation study.

4. Calibration

We want to infer G_{tot}, the value of the overall gain of the TREND electronics system. For this, we used the sky and ground thermal radiations, which are well known. Indeed, apart from transient signals, the signal (which is actually noise for us) that the antenna receives is dominated by the sky

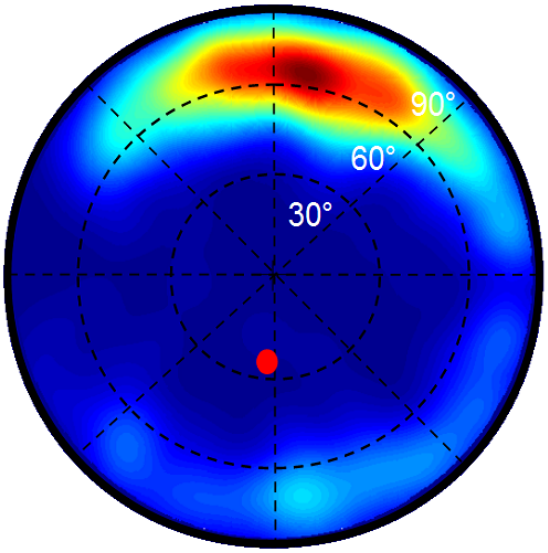

Figure 2: Angular distribution of the 574 air shower candidates selected by the offline analysis. The direction of the geomagnetic field at the experimental site is embodied by a red dot.

and ground thermal radiations,

$$\langle V_{ant}^2 \rangle = \langle V_{sky}^2 \rangle + \langle V_{ground}^2 \rangle . \tag{4.1}$$

$$\langle V_{DAQ}^2 \rangle = G_{tot}^2 \left(\langle V_{sky}^2 \rangle + \langle V_{ground}^2 \rangle \right), \tag{4.2}$$

with

$$\langle V_{sky}^2 \rangle = \frac{R_L}{2} \int_{\Delta\nu} \int_{4\pi} B_\nu(\theta,\varphi,\nu) A_{eff}(\theta',\varphi',\nu) \sin\theta d\theta d\varphi d\nu, \tag{4.3}$$

$$\langle V_{ground}^2 \rangle = k_B \langle G_{ant} T_{ground} \rangle_{4\pi} \Delta\nu R_L. \tag{4.4}$$

The factor 1/2 in equation 4.3 stands for the combination of a monopolar antenna and the unpolarisation of thermal radiations.

The LFmap [6] software allows to compute B_ν, the sky brigthness, as a function of the frequency and of the angles of view in the equatorial coordinate system (see picture 3),

$$B_\nu(\theta,\varphi,\nu) = \frac{2\nu^2 k_B T_{sky}(\theta,\varphi,\nu)}{c^2}. \tag{4.5}$$

The ground black body temperature is $T_{ground} = 290$ K.

We used NEC [7] (Numerical Electromagnetic Code) to compute the effective area A_{eff} and passive gain G_{ant} of the antenna. A_{eff} embodies the antenna response to an incoming electromagnetic wave. It is a function of θ,φ, and ν, respectively the angles of the wave propagation in the antenna framework (prime marks in equations) and the wave frequency. A_{eff} depends on the antenna design, its relative position to the ground, ground characteristics, and impedance match between antenna ($Z_A = R_A + i\chi_A$) and electronic circuit load ($Z_L = R_L + i\chi_L$). G_{ant} is related to A_{eff} with

$$G_{ant}(\theta,\varphi,\nu) = A_{eff}(\theta,\varphi,\nu) \frac{4\pi\nu^2}{c^2}. \tag{4.6}$$

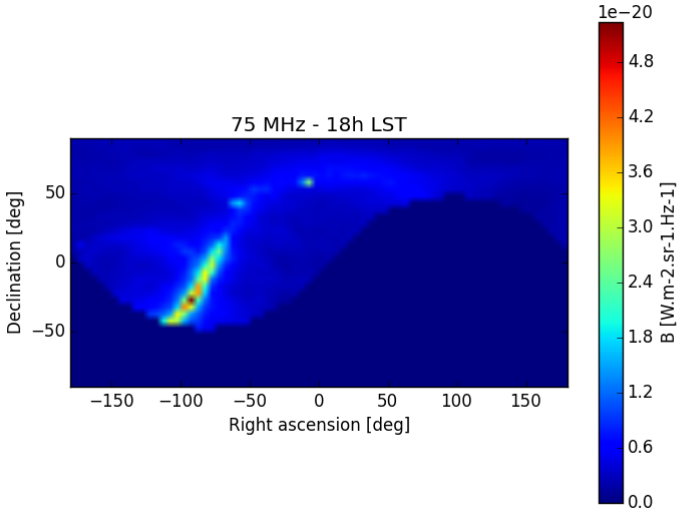

Figure 3: Visible sky brightness at 6 pm LST (Local Sideral Time), computed from LFmap data.

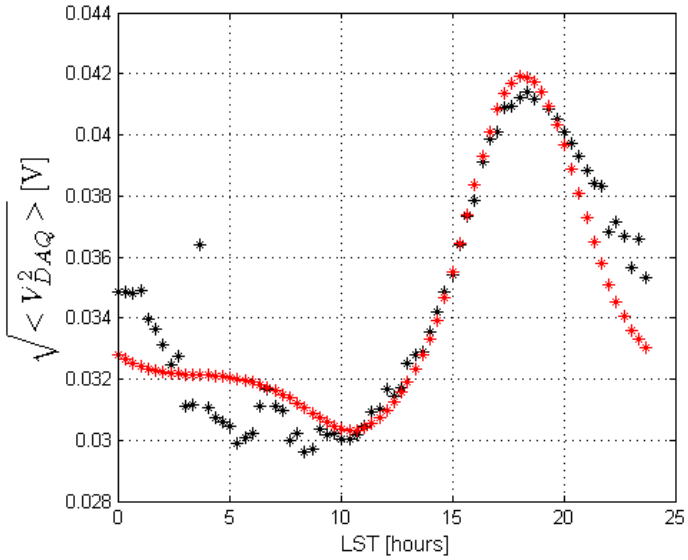

Figure 4: Recorded (black) and expected (red) RMS voltage as a function of LST (Local Sideral Time).

Its mean value on the whole solid angle is 1 in case of impedance matching ($Z_L = Z_A^*$) [4, 5].

Each 20 minutes, the TREND acquisition records random trigger signals in the form of a squared voltage density spectrum. Therefore, for each antenna and for each 20 minutes, we calibrate the value of G_{tot}^2 to ensure that the expected squared voltage $< V_{DAQ}^2 >$ matches the recorded one. Figure 4 represents with black stars the recorded RMS voltage as a function of LST (Local Sideral Time) for one day, for one of the TREND antennas. The expected RMS voltage (red stars) is superimposed, with a constant value of G_{tot}, for the purpose of illustration only. The curves

match at $\pm 10\%$. This means only a scaling parameter (G_{tot}) is required to match the amplitudes and the absolute positions. Thus, this is a validation of our model. However, independent measurements indicate an additional noise ranging between 0% and 20% (see in particular figure 1 of [3]). Indeed, it is easy to conceive that we did not take all the sources of noise into account. Thus, G_{tot} can be overestimated up to 20%. In the following we will therefore consider a range of values for the gain, between $G_{tot}/1.2$ and G_{tot}.

5. Efficiency computation

To compute the efficiency of TREND to detect extensive air showers, we simulated air showers and propagated them into the TREND data acquisition system (antenna, electronic, and trigger conditions), and inserted them in experimental data files, as explained bellow.

The experimental data subset we used in this section ranges from February, 23th, to June, 19th, of 2012, which corresponds to 80 data acquisition days, and for which the data analysis aforementioned has selected 205 air shower candidates. The simulation set is made of 11 energies, between 5.10^{16} and 3.10^{18} eV, with up to $N_{draw} = 10^4$ air showers per energy. The angular distribution of these simulated air showers is uniform over the whole sky. Their core positions on the ground cover a surface S_{draw} large enough to include all the detectable air showers. All the simulated events used in the present analysis are proton induced air showers. A preliminary analyis including iron induced air showers does not show significant differences for the results.

Firstly, using ZHAIRES [8] (Zas, Halzen, and Stanev radio simulation using AIR-shower Extended Simulation), we generated the air showers and their electromagnetic field at each TREND antenna position. Next, we compute each corresponding voltage with NEC. At this stage, we have to insert the simulated events in experimental data files. To do this, for each simulated air shower, we use a random time (taken within the data acquisition time) to choose the insertion file and time position in the file, and apply the electronic chain effects to the raw voltages: frequency filter, electronic gain G_{tot} at the insertion time, digitization, and noise addition (taken from experimental data at the insertion time). Then, if these simulated signals pass the trigger threshold condition, they are inserted in the experimental data file, within really recorded signals.

Afterwards, we analyse the data files with inserted simulated signals, with the same offline program we used to analyse the data (see section 3). The N_{sel} simulated air showers which succeed to be inserted in files and that pass through all the offline cuts are used to compute S_{eff}, the effective surface of TREND for each shower energy and angles, and to finally compute the TREND aperture (in $\mathrm{m}^2.\mathrm{sr}^1$) as a function of the energy, as explained by the following equations,

$$S_{eff}(\theta,\varphi,E) = S_{draw}(\theta,\varphi,E)\frac{N_{sel}(\theta,\varphi,E)}{N_{draw}(\theta,\varphi,E)}, \tag{5.1}$$

$$Ap(E) = \int_{2\pi} S_{eff}(\theta,\varphi,E)\cos\theta\sin\theta d\theta d\varphi. \tag{5.2}$$

Then we get,

$$N_{expected} = \int_{\Delta E} Ap(E)F(E)dE\Delta t, \tag{5.3}$$

with $F(E)$ the cosmic ray flux [9] (in $\mathrm{GeV}^{-1}.\mathrm{m}^{-2}.\mathrm{sr}^{-1}.\mathrm{s}^{-1}$) and Δt the data acquisition duration.

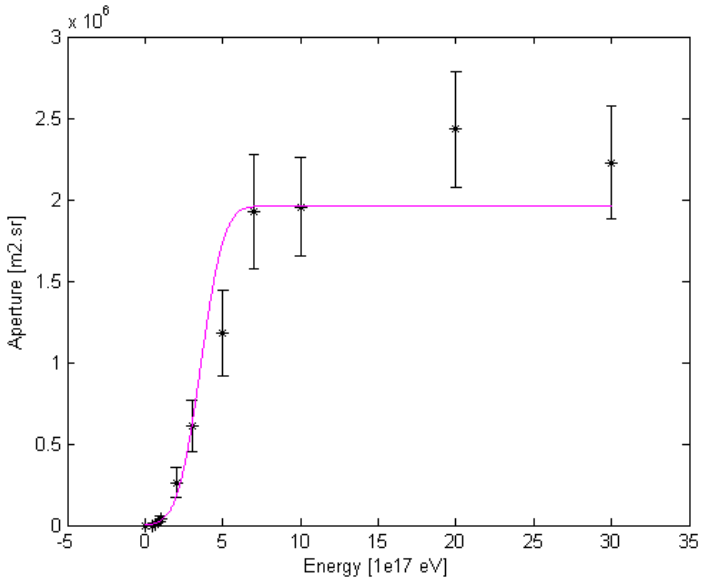

Figure 5: TREND aperture. Error bars are $\pm 1\sigma$.

From this, we obtained the aperture points shown in figure 5, which are fitted with the following,

$$Ap(E) = a.10^6(1+erf((E-b)/c)), \tag{5.4}$$

with $a = 1.02$, $b = 3.62$, $c = 1.67$, and E is in units of 10^{17} eV. Taking into account the G_{tot} uncertainty, we found that $N_{expected}$ is between 159 and 240 for the 80 data acquisiton days. Comparing this result to the 205 effective air shower candidates, we can say that our modelling of extensive air shower radio emission and of the TREND data acquisition system is satisfying.

We also computed the expected angular distribution of the air shower arrival directions. The result is depicted with red lines in figure 6, superimposed on the experimental distribution of selected air shower candidates (in black, also shown in figure 2 for the whole data set). This result shows that air showers have indeed been detected and selected by TREND, while the disagreement between the two distributions indicates we have non neglictable noise contamination, originating from directions where noise sources are observed (large zenith angles and $90^\circ < \varphi < 200^\circ$). The distribution with $G_{tot}/1.2$ involves a noise contamination of about 30%.

It is possible to compute the TREND extensive air shower detection and selection efficiencies from the simulations. We define ε_{det}, the efficiency of the detector, as the ratio of the number of air showers we expect with the real TREND array, to the number we expect with an ideal TREND array. An ideal TREND array has a 100% uptime for all the antennas, a 100% data acquisition live time, and its environment noise is only made of sky and ground radiations. We also define ε_{sel}, the selection efficiency of our offline treatment, as the ratio of the number of air showers we expect after offline selection, to the number we expect before this selection (equivalent to an ideal offline selection which would not cut any air shower). The ideal detector and ideal selection apertures are shown in figure 7, respectively in blue and green. From these curves, we got 2188 to 3279 expected events with the ideal TREND detector and 370 to 561 expected events with the real TREND detec-

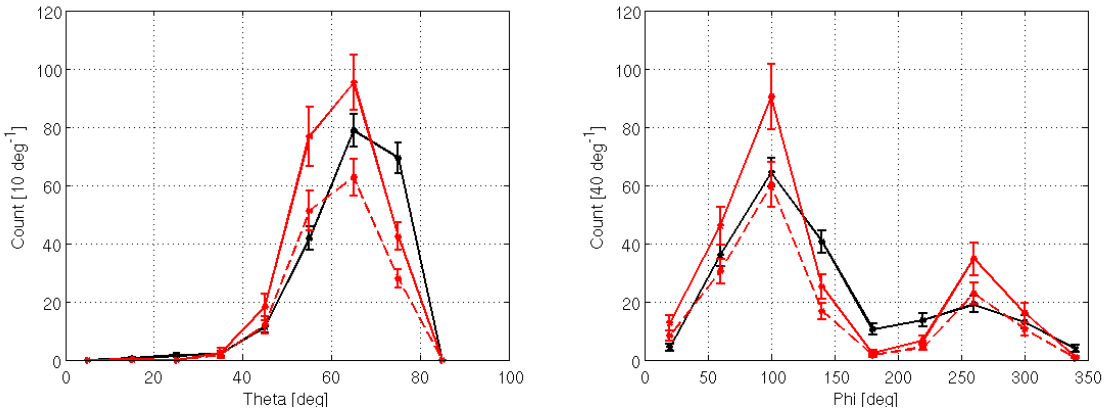

Figure 6: Angular distribution of selected air showers. Experimental candidates in black. Simulated air showers in red. Continuous red line for G_{tot} and dashed red line for $G_{tot}/1.2$. East is at $\varphi = 0°$, North is at $\varphi = 90°$.

tor but with an ideal offline selection, still for 80 data acquisition days. Therefore, $\varepsilon_{det} = 17\%$ and $\varepsilon_{sel} = 43\%$. The latter value shows that, despite very limited means of discrimination (monopolar antennas, layout not suited well for air shower detection), a very good background rejection was achieved with a limited cost for selection efficiency. The very modest value of ε_{det} however shows that the TREND setup suffered from maintenance and reliability issues.

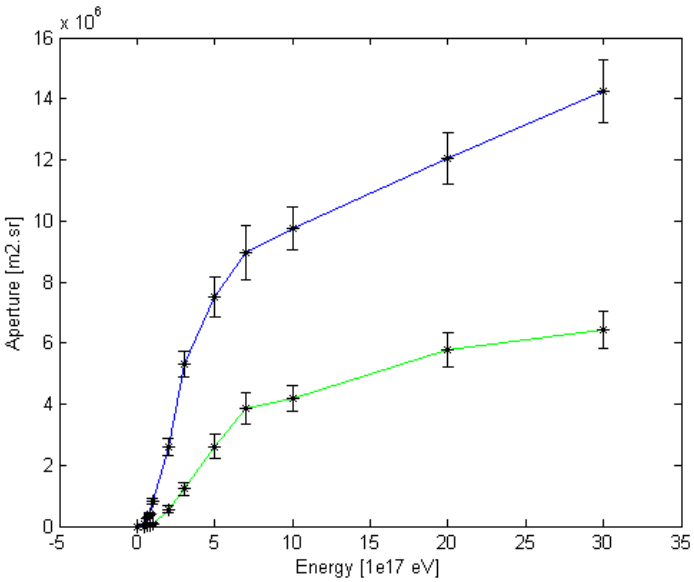

Figure 7: TREND ideal detection (blue) and ideal selection (green) apertures. Error bars are $\pm 1\sigma$.

6. Conclusion

The rate and angular distribution of air shower candidates detected and selected by TREND is compatible with what is expected from simulations. Autonomous radio detection of extenstive air

showers between 5.10^{16} and 3.10^{18} eV was performed by TREND, with a detection efficiency of 17%, an air shower selection efficiency of 43%, and a noise contamination around 30%.

These results are promising for future experiments dedicated to very high energy neutrinos detection such as GRAND. Actually, because of their low flux, large surfaces of detection are required to detect them. To reach a huge surface, one has to reduce the cost and complexity of deployment. Thus, autonomous radio detection seems to be a realistic option.

References

[1] The Pierre Auger Collaboration, "Measurement of the Radiation Energy in the Radio Signal of Extensive Air Showers as a Universal Estimator of Cosmic-Ray Energy," Phys. Rev. Lett. **116** (2016) no.24, 241101

[2] The Tunka-Rex Collaboration, "Radio measurements of the energy and depth of maximum of cosmic-ray air showers by Tunka-Rex," JCAP **01** (2016) 052 doi:10.1088/1475-7516/2016/01/052

[3] D. Ardouin *et al.*, [TREND collaboration] "First detection of extensive air showers by the TREND self-triggering radio experiment," Astropart. Phys. **34** (2011) 717

[4] C. A. Balanis, Antenna theory, analysis and design, Third Edition, A. John Wiley & sons inc. publication (2005).

[5] Warren L. Stutzman, Gary A. Thiele, Antenna theory and design, Third Edition, A. John Wiley & sons inc. publication (2013).

[6] `http://www.astro.umd.edu/emilp/~LFmap`

[7] `http://www.nec2.org/`

[8] E. Zas, F. Halzen, and T. Stanev, Electromagnetic pulses from high-energy showers : Implications for neutrino detection, Phys. Rev. D 45 (1992) 362-376.

[9] `http://pdg.lbl.gov/2017/reviews/rpp2016-rev-cosmic-rays.pdf`